Tissue microstructure characterisation through relaxometry and diffusion MRI using sparse component analysis

Miguel Molina-Romero[1,2], Pedro A Gómez[1,2], Jonathan I Sperl[2], Derek K Jones[3], Marion I Menzel[2], Bjoern H Menze[1]

[1]Computer Science, Technische Universität München, Munich, Germany
[2]GE Global Research, Munich, Germany
[3]CUBRIC School of Psychology, Cardiff University, Cardiff, United Kingdom

Abstract. We introduce a new approach to characterise brain tissue microstructure combining diffusion MRI and relaxometry. The tissue is modelled as a composition of water pools with distinct T2 and diffusivities. Mathematically, we establish a blind source separation framework that we solve using sparse component analysis. Results show that this technique is able to extract distinct diffusion and relaxometry properties of the different water pools.

1 Purpose

Brain tissue microstructure characterisation through diffusion MRI[1,5,9,11] and relaxometry[7] have been a topic of interest for the last 20 years. However, only few works have considered both methods together[6,8]. These techniques have high scanning time requirements and need for regularisation to separate tissue components. In this abstract we integrate the work on tissue characterization from the relaxometry and diffusion perspectives. We present a new approach that does not require regularisation and is less acquisition time demanding. To this end, we use sparse component analysis (SCA)[2] of the diffusion signal to estimate the number of compartments present in the tissue, their T2 decays, volume fractions and diffusivities, as well as the proton density (PD) for each voxel. For the signal model, we assume that 1) the brain tissue contains distinct water pools; 2) there is no water exchange between them; and 3) each pool has a different T2 and diffusivity.

2 Methods

When a diffusion protocol is acquired for a given echo time (TE) the measurement is a linear combination of the diffusion signals from each compartment ($E_i, i = 1, ..., N$ compartments) scaled by the volume fractions (f_i) and the inverse exponential of the ratio between the TE and each $T2_i$ (Eq. 1).

$$S(TE, \Delta, q) = S_0 \sum_{i=1}^{N} f_i e^{TE/T2_i} E_i(\Delta, q). \tag{1}$$

If the same diffusion experiment is repeated for different values of TE, the mixtures of the linear combination of the sources change, producing different signal strengths, according to Eq. 2.

$$\begin{bmatrix} S(TE_1, \Delta, q) \\ \vdots \\ S(TE_M, \Delta, q) \end{bmatrix} = \begin{bmatrix} f_1 e^{TE_1/T2_1} & \cdots & f_N e^{TE_1/T2_N} \\ \vdots & \ddots & \vdots \\ f_1 e^{TE_M/T2_1} & \cdots & f_N e^{TE_M/T2_N} \end{bmatrix} \begin{bmatrix} E_1(\Delta, q) \\ \vdots \\ E_N(\Delta, q) \end{bmatrix}, \tag{2}$$

or equally $X = AS$.

Only the noisy measurements are known (X). However, we are interested in the mixing matrix (A), that only depends on the volume fraction and relaxation properties of the tissue, and the compartmental diffusion sources (S). Typically, this is a blind source separation problem. Approaches based on independent component analysis (ICA) cannot be used since the diffusion sources are not statistically independent. Principal component analysis (PCA) does not offer a good alternative given that the sources are not orthogonal. Therefore, non-negative matrix factorization (NMF) and sparse component analysis (SCA) are the two suitable solutions. NMF is discounted as it requires prior knowledge of the number of compartments. Therefore, SCA is used here. It relies on finding a transform domain where the sources (rows of S) are sparse and disjoint. When these requirements are met, only a few elements in S are non-zero. Then, only one of the sources is active at a time and therefore, the contribution of each specific source to the measured signal can be estimated.

We study this approach by simulating a three compartment tissue made of myelin, intra-extra (IE) axonal water and CSF[7]. The volume fraction for each compartment are based on a fuzzy segmentation with tissue probabilities for grey matter (p_{GM}), white matter (p_{WM}) and CSF(p_{CSF}) [3]. We split the WM and GM probabilities into myelin and IE probabilities by multiply them by a volume of myelin of 11.3% for WM and 3.1% for GM[10] ($p^{WM}_{myelin} = 0.113 p_{WM}$, $p^{WM}_{IE} = 0.887 p_{WM}$, $p^{GM}_{myelin} = 0.031 p_{GM}$, $p^{GM}_{IE} = 0.969 p_{GM}$). Data was simulated using three one-dimension diffusion protocol comprising for 32 equally spaced q-values from 0 to 0.8106 m^{-1}, for TE values of 40, 70 and 80ms. The diffusion sources were generated with Camino[4] using restricted, hindered and free diffusion models for the myelin, IE water and CSF respectively (Fig 2d). Finally, the T2 decays for each compartment were 30ms, 90ms and 2s for myelin, IE and CSF[7]. Signals were mixed using Eq.1 to generate the measurements (X). Then, Rician noise was added up to an SNR of 30 dB at $b = 0$. Finally, the signals were disentangled with SCA using a Gaussian wavelet transform. This type of wavelet has a Gaussian envelop that is similar to the measured 1D diffusion signal thus, transformed coefficients are sparse and, as disjoint as different their diffusion coefficients are.

3 Results

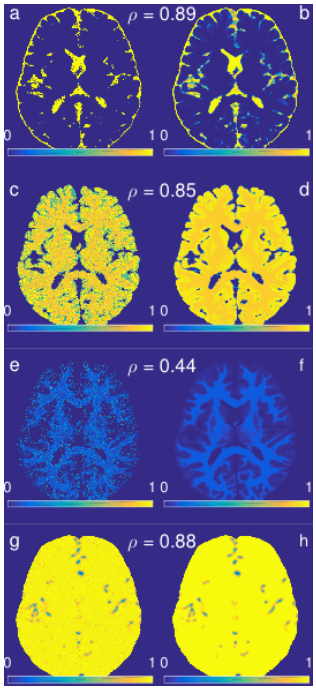

Fig. 1. Comparison between the noisy estimates (left) and the noise free ground truth (right).

Fig. 1 presents the volume fractions for CSF (a), IE (c) and myelin (e) compared to their reference tissue type probabilities (b, d, f). The normalised PD is shown (Fig. 1g) in comparison to the ground truth (Fig. 1). The distribution of the values in Fig. 1(a, c, e) are presented in Fig 2b along with the disentangled T2 (Fig. 2a) and diffusivities (Fig. 2c) for each compartment. The probability values in Fig. 2 correspond to the histograms of the parameter for each compartment and cannot be compared to others.

4 Discussion

High correlation levels between the estimates and the references for CSF, IE and PD are shown in Fig. 1(a-b, c-d and g-h) indicating a good level of separation for the volume fractions. However, myelin correlation level (Fig. 1e-f) is lower, pointing out the difficult detection of short T2 decay components within the limits of feasible TE values. Fig. 2b shows the histogram distribution volume

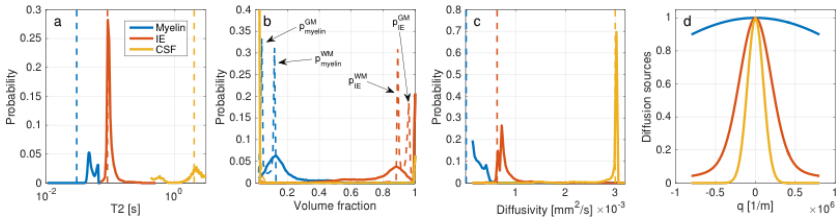

Fig. 2. Histograms for T2 values (a), volume fractions (b) and diffusivities (c). Dashed lines mark the reference values while solid lines correspond to the estimates. Diffusion signal sources are shown in (d)

fractions. The myelin and IE fractions are correctly extracted for WM, while for GM the peaks are shifted to 0 and 1 respectively, due to the low level of myelin present in that tissue. The T2 distribution (Fig. 2a) presents a bias between 15 to 30ms for myelin, while accurately capture the reference value for IE and CSF. The diffusivity also shows a good agreement between estimates and reference for the three compartments. Nevertheless, the small amount of myelin signal in the mixture yields a low SNR disentangled source preventing for a reliable diffusivity estimate for this compartment.

5 Conclusions

To the best of our knowledge, this is the first attempt to use SCA to characterise tissue microstructure using diffusion MRI. Although this proof-of-concept is subject to further improvement, the results presented here indicate that this technique is able to disentangle multiple compartments and thus, can be used to study the T2, volume fractions, diffusion and PD properties of the tissue microstructure simultaneously. An alternative approach to disentangle relaxometry and diffusion information is presented in[6]. Although, unlike SCA it relies on heavy regularisation. Finally, since A is independent of the diffusion signal, this technique can be applied to any diffusion protocol. This paves the way for potential applications such as free water elimination or estimation of the compartmental propagator.

References

1. Assaf, Y., Basser, P.J.: Composite hindered and restricted model of diffusion (CHARMED) MR imaging of the human brain. NeuroImage 27, 48–58 (2005)
2. Boÿll, P., Zibulevsky, M.: Underdetermined blind source separation using sparse representations. Signal Processing 81, 2353–2362 (2001)
3. Collins, D.L., Zijdenbos, a.P., Kollokian, V., Sled, J.G., Kabani, N.J., Holmes, C.J., Evans, a.C.: Design and construction of a realistic digital brain phantom. IEEE transactions on medical imaging 17(3), 463–468 (1998)

4. Cook, P.A., Bai, Y., Nedjati-Gilani, S., Seunarine, K.K., Hall, M.G., Parker, G.J., Alexander, D.C.: Camino: Open-Source Diffusion-MRI Reconstruction and Processing. Proc Intl Soc Mag Reson Med (2014)
5. Ferizi, U., Schneider, T., Witzel, T., Wald, L.L., Zhang, H., Wheeler-Kingshott, C.A., Alexander, D.C.: White matter compartment models for in vivo diffusion MRI at 300mT/m. NeuroImage 118, 468–483 (2015)
6. Kim, D., Kim, J.H., Haldar, J.P.: Diffusion-Relaxation Correlation Spectroscopic Imaging (DR-CSI): An Enhanced Approach to Imaging Microstructure. Proc Intl Soc Mag Reson Med (2016)
7. Mackay, A., Laule, C., Vavasour, I., Bjarnason, T., Kolind, S., M7dler, B.: Insights into brain microstructure from the T 2 distribution. Magnetic Resonance Imaging 24, 515–525 (2006)
8. Peled, S., Cory, D.G., Raymond, S.A., Kirschner, D.A., Jolesz, F.A.: Water diffusion, T(2), and compartmentation in frog sciatic nerve. Magnetic resonance in medicine 42(5), 911–8 (1999)
9. Stanisz, G.J., Wright, G.A., Henkelman, R.M., Szafer, A.: An analytical model of restricted diffusion in bovine optic nerve. Magnetic Resonance in Medicine 37(1), 103–111 (1997)
10. Whittall, K.P., Mackay, A.L., Graeb, D.A., Nugent, R.A., Li, D.K.B., Paty, D.W.: In vivo measurement ofT2 distributions and water contents in normal human brain. Magnetic Resonance in Medicine 37(1), 34–43 (1997)
11. Zhang, H., Schneider, T., Wheeler-Kingshott, C.A., Alexander, D.C.: NODDI: Practical in vivo neurite orientation dispersion and density imaging of the human brain. NeuroImage 61(4), 1000–1016 (2012)